# Electrical and Draping Performance of 3D-Printed Conductive Composites Integrated with Textile Fabric

Solmon, R and Fayazbakhsh, K*
Department of Aerospace Engineering, Toronto Metropolitan University, Toronto, Ontario M5B2K3, Canada
*Corresponding author: kazem@torontomu.ca; Tel: (+1) 416-979-5000 ext. 556414; fax: (+1) 416-979-5056; https://orcid.org/0000-0003-3963-8282

**Keywords**: *3D-printing, Conductive Composites, Wearable Technology*

In the current field of wearable technology, silver yarns are used to provide electrical conductivity to non-conductive textile fabrics required for monitoring and measurement. This work aims to provide an alternative to silver yarn by exploring innovative methods to integrate 3D-printed circuitry onto textile fabrics to offer an ideal solution for prototyping textile-based wearable technology products. For the first time, different conductive composite filaments were investigated for both improved electrical conductivity and drapability. Specimens were fabricated by 3D printing electrically conductive material on a textile fabric between two disconnected squares made of knitted silver yarn. Electrical conductivity and drapability were two design objectives. 3D printed samples were made from off-the-shelf conductive composite filaments: two carbon black/PLA filaments and one copper/polyester filament. All samples are manufactured using a Material Extrusion (MEX) 3D printer. The impact of trace patterns, width, and thickness on electrical conductivity on a hard surface and textile fabric was evaluated along with drapability. The copper/polyester trace integrated onto the textile through 3D printing was found to have electrical and draping performance similar to the reference textile fabric made with silver yarn. The S-pattern geometry with a 2.5 mm trace radius, 4 mm width and 1.5 mm thickness was best for electrical performance, possessing a resistance of 3.58 Ω/cm and draping coefficients of 45.3 % along the trace and 61.1 % across the trace. The S-pattern geometry with the same width and thickness, but a 5mm trace radius, exhibited a slightly higher resistance of 4.76 Ω/cm, but lower draping coefficients of 35.8% and 57.7 % along and across the trace, respectively. This made it a better choice for applications where enhanced drapability is critical.

**Fibers and Polymers**

**https://doi.org/10.1007/s12221-025-01137-2**

# 1 Introduction

The field of additive manufacturing from conductive composite filaments (CCFs) has advanced greatly over the last couple of decades. Some of the first experiments on this topic involved the additive manufacturing of silver conductive inks [1, 2]. Over the next decade, these experiments quickly advanced to 3D printing CCFs made from various polymers. Polylactic acid (PLA) is a commonly used polymer due to its biocompatibility and has been investigated for electrical performance when combined with different conductive fillers [3, 4]. Filler type, weight content, aspect ratio, and orientation impact its electrical conductivity, which is governed by the mixture role. The percolation threshold is specified as the critical filler content at which the electrical conductivity increases several orders of magnitude. The filler-to-filler contact at high concentrations allows the fillers to form a conductive mesh, assisting with charge transport [5]. While high filler contents are beneficial to achieve high electrical conductivity, it comes at the cost of reducing manufacturing flexibility and increasing fabrication cost. 3D printing commercially available CCFs is more straightforward compared to developing a new filament. For this reason, many researchers focus on characterizing the electrical performance of commercially available CCFs [6-9].

A drawback of silver yarn is the expensive equipment replacements or modifications that are required to incorporate silver yarn into the manufacturing process [10, 11]. By contrast, integrating 3D printed traces with textile fabrics allows companies to prototype, and potentially manufacture, e-textile products using previously acquired knitting equipment. Therefore, 3D printing conductive traces on textile fabrics can offer a more cost-effective alternative to the expensive equipment changes needed for integrating conductive material into textile fabrics. In addition to the need for costly and specialized equipment, there are concerns regarding materials cost and sustainability. Products that utilize silver also rely on supply chains from the precious-metal industry with a high environmental impact and lack circular recycling routes which aim to minimize waste and maximize resource usage [12]. The brittleness of silver also leads to mechanical degradation during wash cycles, such as micro-cracking and abrasion, which reduce electrical performance and necessitate more frequent replacement, further increasing material waste [13].

Wearable technologies provide numerous benefits across various applications, including preventative and personalized healthcare [14, 15], education [16, 17], and sports [18, 19]. Techniques for integrating electrical properties to textile-based wearable technology have evolved from using conductive wires and fibers [20, 21] to developing conductive textile structures [22, 23]. Recent studies have investigated newer integration techniques including integrating electrically conductive inks [24, 25] and CCFs using additive manufacturing technology [26, 27]. 3D Printing CCFs on textile fabric has allowed for many innovative approaches to manufacturing flexible electronic components, such as sensors, circuits, and interconnects [8, 26]. Commercially available PLA based CCFs were commonly chosen when 3D printing on textile fabric and demonstrated good adhesion [28]. On the other hand, thermoplastic polyurethane (TPU) based CCFs showed some difficulty printing on textile fabric along with inconsistent electrical performance [26, 29]. For this reason, two PLA-based conductive composites (3DKonductive and Protopasta) and one polyester-based material (Electrifi) were chosen here. Previous research has investigated Protopasta printed on conductive textile fabric. However, this study had a very limited scope and did not compare different filaments [30]. Work with Electrifi has been carried out to investigate its electrical performance, but no research has investigated 3D printing this material onto a textile fabric. Previous work has been conducted using thermo-compression to integrate 3D printed Electrifi structures onto textile fabric [8].

Although many papers have investigated the electrical performance and adhesion of CCFs integrated onto textile fabric through 3D printing, none of these papers investigated the drapability of the resulting structure. When integrating 3D printed structures with textile fabric, drapability is an important characteristic for textile

performance. Drapability is defined as the ability of the textile to deform under the gravity force which is crucial for the aesthetics and functionality of 3D printed textile structures [31]. If a material has limited drapability, it may not be appropriate for specific wearable technology applications, which require high flexibility from the textile. The drapability of 3D printed TPU textile structures have been investigated, but these structures were not integrated with textile fabric [31, 32]. Spahiu et al. [33, 34] has researched the impact of small 3D printed PLA shapes on the draping performance of a textile fabric. However, no experiments have explored the effect of larger 3D printed geometries made from different conductive materials spanning across a textile fabric. Examining draping performance in this scenario is crucial for identifying the best CCFs to integrate with textile fabric for wearable technology applications. Table 1 summarizes the best experimental results from the literature on electrical performance of 3D printed structures integrated with textile fabric and draping performance of 3D printed textiles. In addition, the last row provides the results from this study for a simple comparison with the literature. No research work has investigated both the electrical and draping performance of a conductive trace 3D printed on textile fabric.

**[insert Table 1 here]**

Integrating 3D printed CCF traces with textile fabrics using MEX technology has the potential to offer a less expensive solution for incorporating conductive material with textiles compared to silver yarn. This is especially useful for prototyping textile-based wearable technology products requiring flexible and conductive components. This integration technique may also have manufacturing applications in the near future as automated 3D printing technology progresses. However, to be considered a viable substitute the electrical and draping performance of the 3D printed traces integrated with textile fabric should be comparable to silver yarn.

This study investigated the electrical performance and drapability of commercially available CCFs integrated with textile fabric to determine if they could be an appropriate substitute for conductive silver yarn commonly used in wearable technology applications. Electrical performance was characterized by comparing the resistance per unit length, also called normalized resistance, of different CCF traces printed on a rigid surface. The two CCFs with the lowest resistance per unit length were then integrated with textile fabric to observe how their electrical performance and drapability compared to conductive silver yarn.

# 2 Experimental

## *2.1 Materials*

To compare the integration of 3D printed CCFs to the conductive silver yarn baseline, textile fabric samples were made by Myant Inc., a wearable technology company based in Mississauga, Ontario, Canada. The textile fabric samples were made in a full needle knit structure using polyester yarn with 78 decitex and 48 filaments per yarn and silver yarn with 240 µm diameter. These samples were knitted in the shape of a square with 1 mm thickness and 150 mm side lengths. These samples had two conductive squares with 10 mm side lengths, which were knitted using the silver yarn and integrated into the middle of each textile fabric 10 mm away from each end (Figure 1). The conductive squares in the baseline samples were connected by a silver yarn thread embedded between the polyester base material using a proprietary knitting technique and these samples weighed between 5.55 g and 5.60 g. In experimental textile fabrics, 3D printed conductive composite traces replaced the connecting silver yarn thread, which allowed for comparison to the baseline in terms of electrical performance and drapability.

**[insert Figure 1 here]**

Three commercially available thermoplastic CCFs were selected for testing. These filaments were chosen based on the specific volume resistance reported by the manufacturer. Two conductive filaments used a carbon black filler to improve conductivity. These two carbon black/PLA filaments were 3DKonductive (3DK) (3DK.Berlin, Berlin, Germany), which had a reported resistivity of 24 Ω.cm for a printed structure [35], and Protopasta Conductive PLA (Protoplant Inc., Vancouver, USA), which had a reported resistivity of 30 Ω.cm in the x/y-direction and 115 Ω.cm in the z-direction [36, 37]. The last commercially available CCF used was Electrifi (Multi3D, Middlesex, USA), which used copper as its filler. This copper/polyester composite had a reported resistivity of 0.006 Ω.cm [38, 39]. All filaments were 1.75mm in diameter and 3D printed with a 0.8 mm nozzle diameter. This nozzle size was chosen since it was larger than the minimum diameter required to prevent clogging from the conductive filler particles, in accordance with the manufacturer's specifications. Table 2 summarizes the three conductive filaments used in this study.

**[insert Table 2 here]**

In the following sections, trade names of the filaments were used for better identification and simplified naming convention of specimens.

## *2.2 Specimen manufacturing*

A Creator Pro 2 (Flashforge, Jinhua, China) 3D printer was used to manufacture the 3D printed conductive composite traces. To ensure the print settings for each material were acceptable and the desired geometries could be manufactured successfully, a geometric capability assessment (GCA) was carried out on each material following the ISO/ASTM 52902:2019(E) standard [40]. 3DK and Protopasta did not require improvement of the 3D printing process parameters and were fabricated successfully with the manufacturer's recommended settings. However, the Electrifi material was challenging to 3D print, which agrees with other research utilizing this material [9]. This finding signifies that the ease of manufacturing needs to be considered beside electrical performance of conductive filaments.

The smallest detail that could be consistently produced by the 3D printer was a 2 mm pin in the resolution pin model from the standard. Therefore, this was chosen as the smallest trace width, and the width was doubled to give a variety of cross-sectional areas. The trace thickness was selected to be between 1 and 2 mm so that sufficient electrical performance is provided without severely inhibiting the bending and consequently the draping performance. Once the GCA was performed and each CCF could be 3D printed consistently, the trace designs were finalized in FreeCAD, an open-source parametric 3D modeler. Traces were designed with varying cross-sectional areas (CSAs) to investigate how changes in geometry affect the electrical performance of each material. These samples were also used to compare the resistivity (the inverse of conductivity) of the 3D printed traces to the unprinted feedstock material. Two categories of traces with different geometries were designed: straight-line (SL) and S-pattern (SP) traces. SL and SP trace geometries were compared to determine the differences in electrical and draping performance. SP traces were expected to have worse electrical and better draping performance. However, the degree of impact the geometric changes had on each performance metric remained unknown. The SL traces were designed with different CSAs, including widths of 2, 3, and 4 mm, thicknesses of 1 and 2 mm, and fillets of 0, 1, and 2 mm (Figure 2a & b). Each CSA was 3D printed once in an SL trace with each CCF using the Creator Pro 2 (Flashforge, Zhejiang, China) 3D printer and compared to determine the two most conductive filaments. These samples were fabricated on painter's tape with no pre-extrusion and no raft to closely resemble the conditions that would be used when printing on the textile fabric. Two variations of the SP traces were designed from the most conductive geometries of the SL trace to maximize electrical performance. One geometry of the SP trace had a 2.5 mm trace radius with ten 180° turns and two 90° turns, while the other SP trace had a 5 mm trace radius with six 180° turns and two 90° turns (Figure 2c & d). The two most conductive materials were integrated with textile fabric in SL and SP geometries for comparison with the baseline. Both the SL and SP trace geometries had the same end-to-end distance of 115 mm, and the samples were named based on their distinct geometries. For example, an Electrifi SL trace of 4mm width, 2mm thickness, and 1 mm fillet would be denoted as E-SL-W4T2F1. For SP trace geometries, "SL" was replaced with either "SP-TR2.5" or "SP-TR5", i.e., E-SP-TR2.5-W4T2F1. The trace geometry was so narrow it did not allow for an infill between the rectangular ends of the trace. However, the structure of the rectangular ends themselves was affected by the infill percentage, so an infill of 100% was used to minimize gaps that would inhibit electrical performance. The 3D printing process parameters for each material are presented in Table 3.

**[insert Figure 2 here]**

**[insert Table 3 here]**

Experimental textile samples were prepared from the two filaments with the best electrical performance when 3D printed on painter's tape, specifically P-SL-W4T2 and E-SL-W4T1.5. These samples were prepared by printing the best-performing CSA of each filament in SL and SP geometries. Three SL traces and two of each SP trace were printed onto the experimental textile fabric samples resulting in seven samples for each material. The 3D printing process was modified to overcome challenges with alignment and the textile fabric's extra thickness. To align the textile fabric, a thin strip of painter's tape was placed in the centre of the build platform running across the x-axis, and four 41 mm foldback clips were used to secure it to the platform (Figure 3). If the nozzle was caught on the textile during a print, the spacing between the nozzle and textile fabric was increased by 0.05mm increments until the nozzle no longer contacted the textile fabric.

**[insert Figure 3 here]**

### *2.3 Resistance measurement*

Resistance measurements were taken using the 2-point method with two multimeters, a Neoteck$^{TM}$ (Taiwan, China) XL830L and Mastercraft (Vonore Tennessee) 052-0060-2. The 2-point method of measuring resistance was chosen due to the negligible contact resistance of silver yarn. The 2-point method was carried out by placing one probe from the multimeter on each silver pad and applying even pressure until the resistance measurement stabilized. Length was measured with Vernier calipers (Accusize, Ontario, Canada) between the interior edges of the silver pads.

Conductive trace geometries 3D printed on painter's tape required the application of silver conductive epoxy 8330S (MG Chemicals, Ontario, Canada) to the rectangular ends. This was done to negate the effects of contact resistance and is common practice in the literature measuring the electrical performance of 3D printed filaments [7]. These samples were cured at 65 °C for 2 hours in a dehydrator (Noztek, Shoreham-By-Sea, England), then cooled to room temperature before the resistance was measured (Figure 4).

**[insert Figure 4 here]**

The two resistance measurements were recorded, averaged, and divided by the end-to-end distance in cm to determine the resistance per unit length of each trace, also referred to as normalized resistance. These values, which were in units $\Omega$/cm, could be multiplied by the CSA of all 15 SL traces to estimate the resistivity for each material in $\Omega$.cm according to Equation 1 [41].

$$\rho = \frac{ra}{l} \quad (1)$$

Where, $\rho$ is restivity, $r$ is resistance, $a$ is CSA, and $l$ is trace length. The resistivity reported by the supplier was compared to the feedstock filament and 3D printed traces to analyze the electrical performance of the three CCFs. Normalized resistance was compared between traces 3D printed on painter's tape and textile fabric to determine how 3D printing on textile fabric affects the electrical performance. Traces 3D printed on textile fabrics were also compared to the baseline textile fabric made with silver yarn to establish if any experimental textile could achieve similar performance.

### *2.4 Drapability measurement*

Drapability can be measured in different ways, and the method of measurement has changed over time. In current research, comparing the draped and undraped areas of a structure, through a parameter called draping coefficient (DC), has been accepted as an appropriate methodology [31, 32]. Therefore, the *DC* of the baseline and experimental samples were calculated according to the Equation 2 [31, 32].

$$\frac{draped\ area}{undraped\ area} \times 100 = DC \quad (2)$$

To find the *draped* and *undraped area* for each sample, 3D scans were taken using the handheld laser scanner (HandyScan 3D, Creaform Inc., Lévis, Canada). For the undraped configuration, the textile was laid flat on the scanning surface. For draped configurations, the textile was placed over a 50 mm tall and 5 mm wide pole. The height of the pole was selected to have stable draping configurations during the measurement process. The DC was measured in two configurations to determine the effect of the 3D printed trace on the textile fabric's draping performance in different orientations. These configurations included draping along the trace and draping across the trace, the latter can be seen in Figure 5. This figure also demonstrates how experimental samples were taped down when drapability was measured across the trace to simulate a weighted draping measurement [32]. This was necessary since the 3D printed traces were resistant to unassisted draping across the trace. Once all the 3D scans were obtained, the top view images of the samples were processed to make the background black and the sample white (Figure 6). MATLAB was used for pixel-counting, which assigned a numerical value to the white area in the image, allowing the DC to be calculated using Equation 2.

**[insert Figure 5 here]**

**[insert Figure 6 here]**

# 3 Results & Discussion

## *3.1 Electrical Performance*

### *3.1.1 Resistivity of Conductive Composite Filaments*

The resistivity of the three CCFs was compared in Figure 7 based on the supplier reported resistivity [35-39], feedstock filament, and 3D printed traces. Recall that 3DK and Protopasta are carbon black/PLA filaments, and Eletrifi is a copper/polyester feedstock. Although the suppliers reported similar resistivity for 3DK and Protopasta, the measured resistivity of 3DK was an order of magnitude higher than expected. Protopasta feedstock and 3D printed traces had lower resistivity than the supplier reported values for 3D printed structures, and Electrifi had resistivity two orders of magnitude higher than the supplier reported value. This could be attributed to a high batch-to-batch variability in the feedstock due to non-uniform particle size, dispersion, and infill percentage. This was observed by Nowka et al. [42] where they explored multiple filaments for their electrical performance, including Electrifi. The 3DK and Protopasta increased in resistivity after 3D printing, which was a common trend observed by other researchers of conductive filaments [26, 29, 30]. However, the Electrifi CCF decreased in resistivity, which was a less common trend but has been reported in research done by Silvestre et al. [27]. One standard deviation for the 3D printed traces is represented by the error bars in Figure 7. These error bars demonstrate that the structure of the 3DK and Electrifi traces had high variability compared to the Protopasta traces, which had consistent electrical performance across all averaged trace geometries. Equation 1, which was used to calculate resistivity, describes an ideal relationship that is only partially satisfied for 3D printed traces. The two main assumptions are a simple geometry with a consistent CSA and a homogenous material. The 3D printed SL traces are simple geometries but are not completely homogenous materials since 3D printed structures have anisotropic properties [4]. Therefore, changes in structure relating to anisotropy and porosity between different CSAs would change the calculated resistivity of the trace. If there is low variability for the resistivity between different CSA traces, it demonstrates a consistent 3D printed structure is formed across all CSAs for that material.

PLA and polyester are insulating materials and have an electrical conductivity of around $5 \times 10^{-9}$ S/m [43, 44]. Electrifi had the lowest resistivity out of all three CCFs, with values of 0.626 Ω.cm for the feedstock filament and 0.138 Ω.cm for the 3D printed traces. These correspond to electrical conductivity of 160 and 725 S/m, which is close to the lower level of electrical conductivity for conductive materials of 1000 S/m. Protopasta values for the filament and 3D printed trace were, respectively, 6.30 Ω.cm (15.9 S/m) and 14.6 Ω.cm (6.85 S/m). This is in the range of 1-100 S/m for typical conductive composites [5]. 3DK values for the filament and 3D printed trace were 158 Ω.cm (0.633 S/m) and 486 Ω.cm (0.206 S/m), respectively.

**[insert Figure 7 here]**

### *3.1.2 Effect of Trace Geometry on Electrical Performance of 3D Printed Traces*

When 3D printing a trace of equal length with decreasing CSA, the resistance was expected to decrease according to the relationship in Equation 3, which is Equation 1 rearranged to solve for resistance.

$$r = \frac{\rho l}{a} \tag{3}$$

Where $r$ is trace resistance, $\rho$ is resistivity, $l$ is trace length, and $a$ is CSA. This relationship should hold true for simple geometries and homogeneous materials. Although the SL traces are simple geometries, they are 3D printed structures which have anisotropic properties. Therefore, deviations from the relationship in Equation 3 indicate that factors such as homogeneity can substantially affect the resistance of a 3D printed trace.

The effects of trace geometry on the normalized resistance of each 3D printed CCF are presented in Figure 8, where CSA decreases from the left to the right. The 3DK CCF had the worst electrical performance and did not follow the expected pattern of increasing normalized resistance with decreasing CSA. Although the best performing 3DK trace geometries were at larger CSAs, the worst performance was recorded at 4 $mm^2$ instead of the smallest CSA of 1.57 $mm^2$. The 3DK traces seemed to be more sensitive to the width of the trace instead of the overall CSA, indicating that properties such as anisotropy and porosity change with different trace geometries. The Protopasta CCF had the second-best electrical performance, with a normalized resistance one to two orders of magnitude below the 3DK traces. The Protopasta traces followed the expected trend with resistance increasing as CSA decreased, showing a consistent structure was formed across all trace geometries. The Electrifi traces demonstrated some anomalies, and the best performing trace geometry was found at CSAs other than the largest. Similar to 3DK, the width of the trace had a bigger effect than the CSA, indicating the trace structure changes across different geometries. The effect of fillets on electrical performance was the most prominent when comparing SL-W4T1F1 to SL-W3T1, with CSAs of 3 $mm^2$, and SL-W3T1F1 to SL-W2T1, with CSAs of 2 $mm^2$. Fillets were found to lower the normalized resistance of the trace for the same volume of 3D printed material. The two best performing materials were Protopasta and Electrifi, with respective trace geometries of SL-W4T2 and SL-W4T1.5. Their normalized resistance values were 185 $\Omega$/cm for the P-SL-W4T2 sample and 0.791 $\Omega$/cm for the E-SL-W4T1.5 sample.

**[insert Figure 8 here]**

### *3.1.3 Electrical Performance of 3D Printed Traces Integrated with Textile Fabric*

The 3D printed CCFs with the best electrical performance were Protopasta and Electrifi, as seen in Figure 7. The best performing 3D printed SL trace geometries for these materials were found in Figure 8. These two CCFs were 3D printed onto experimental textile fabric samples for comparison with samples printed on painter's tape and the baseline textile fabric. For Protopasta, P-SL-W4T2, P-SP-TR2.5-W4T2, and P-SP-TR5-W4T2 were selected, while for Electrifi E-SL-W4T1.5, E-SP-TR2.5-W4T1.5, and E-SP-TR5-W4T1.5 trace geometries were used.

The analysis of the Protopasta CCF demonstrated in Figure 9, which uses a logarithmic scale for normalized resistance, revealed some interesting trends. The Protopasta traces 3D printed on painter's tape had practically the same normalized resistances as traces 3D printed on textile fabric. Comparing SL and SP traces revealed the SL Protopasta traces had a lower normalized resistance than the SP traces when 3D printed on both the painter's tape and textile fabric surfaces. This was expected since the SL and SP trace resistances were normalized across the same end-to-end distance, and SP-TR2.5 and SP-TR5 traces had path lengths of 183 mm and 197 mm. These path lengths were 1.59 and 1.71 times longer than the 115 mm path length of the SL trace. However, the measured normalized resistances of the P-SP-TR2.5-W4T2 and P-SP-TR5-W4T2 traces were more than 1.95 times larger than the P-SL-W4T2 traces. Therefore, the normalized resistances for the Protopasta SP traces were higher than expected, based on proportional trace length. According to these results, the 3D printing of the nonlinear trace path was found to have an adverse effect on electrical performance for this CCF. This behavior reveals fabricating different trace geometries can affect the microstructure and performance of the 3D print, even when using the same 3D printing process parameters and trace CSA. Overall, the Protopasta traces 3D printed on textile fabric performed two orders of magnitude worse compared to the baseline textile fabric made with silver yarn. The P-SL-W4T2 sample had a

normalized resistance of 176 Ω/cm compared to the baseline textile fabric with a normalized resistance of 3.85 Ω/cm.

**[insert Figure 9 here]**

The normalized resistance of Electrifi traces 3D printed on painter's tape was compared with traces 3D printed on textile fabric in Figure 10. The Electrifi traces did not follow the same pattern as the Protopasta and demonstrated an increase in normalized resistance when 3D printing on textile fabric compared to the painter's tape, which was more rigid. This difference could be attributed to the Electrifi filament extruding at lower temperatures than the Protopasta filament. The lower temperature extrusion requires less time to solidify, which may limit the penetration of Electrifi into the gaps between the knitted silver yarn conductive squares, increasing contact resistance.

When Electrifi was 3D printed on painter's tape, SL traces exhibited lower normalized resistance compared to SP traces. However, on textile fabric, SL traces had higher normalized resistance than SP traces, indicating differences in homogeneity and anisotropy. The increased normalized resistance in SL traces 3D printed on textiles suggested detrimental changes in internal structure, likely due to the trace geometry affecting the 3D printer's nozzle speed. SL traces allowed for the 3D printer to reach maximum nozzle speed due to their linear path. Comparatively, SP traces required many directional adjustments, resulting in slower nozzle speeds. When 3D printing on textile fabric, the slower nozzle speed led to less deformation and a more consistent printing surface, benefiting the electrical performance of these traces. The E-SP-TR2.5-W4T1.5 and E-SP-TR5- W4T1.5 trace geometries 3D printed onto textile fabric had normalized resistances of 3.58 and 4.76 Ω/cm, respectively, while the baseline textile fabric had a normalized resistance of 3.85 Ω/cm. This demonstrated that 3D printed Electrifi traces can achieve similar electrical performance to silver yarn when integrated with a textile fabric.

**[insert Figure 10 here]**

In wearable technology use-cases, long-term resistance drift is common due to mechanical stress and environmental exposure. Flowers et al. [6] demonstrated that the resistance of Electrifi Cu/polyester traces increased after the first few bending cycles and then demonstrated stable resistance and did not fracture after 500 cycles bending the trace up to 180°. Copper and polyester can both exhibit performance degradation due to environmental exposure. Copper will oxidate forming non-conductive and semiconductive portions, reducing the electrically conductive CSA and increasing resistance [45, 46]. Polyester will degrade due to high temperatures and excessive moisture [47, 48], which leads to a loss of mechanical integrity and deforming the matrix and disrupting conductive paths. Polyester's moisture permeability along with its susceptibility to degrade due to water exposure make it an environment likely to accelerate the corrosion of the copper filler [48]. Options like dual material 3D printing and surface modification to add a protective layer to the copper/polyester should be investigated and utilized to help mitigate long-term resistance drift and reduced performance over time in industrial applications. These protective treatments could also assist in chemical resistance for washing.

### *3.2 Drapability Results*

Comparison of drapability in Figure 11 revealed interesting differences between the Protopasta, Electrifi and baseline textile samples. The baseline textile fabric demonstrated a DC of 41.9% along the silver yarn trace and 50.4% across the trace. This could be due to the difference in structure between the silver yarn trace and the rest

of the knitted textile or the anisotropic draping properties of the knitted structure. Both the Protopasta and Electrifi traces integrated with textile fabrics were able to achieve similar DCs to the baseline when draped along the trace. In this scenario, the stiffness of the 3D printed trace has minimal impact on the draping configuration, as demonstrated by Figure 12a and b. In some instances, 3D printed trace geometries draped along the trace had lower DCs than the baseline textile fabric. This was caused by the stiffness of 3D printed trace allowing the textile fabric to fold under the trace, instead of along the surface of the 3D scanning platform (Figure 12c). Since less textile fabric was draped along the scanning platform, the draped area decreased, resulting in a lower DC.

The Protopasta and Electrifi traces 3D printed on textile fabric displayed a large difference in drapability across the trace (Figure 11). Comparing the DC across the trace for SL geometries revealed the Protopasta trace was too stiff to be draped in this direction, while the Electrifi sample could be measured. Compared to SL traces, the SP geometries decreased the DC for both CCFs across the trace. The Electrifi traces 3D printed on textile fabric displayed draping performance much closer to the baseline sample. This variation in drapability stems from the difference in material properties and thickness of 3D printed Protopasta and Electrifi traces. The 3D printed trace geometry with the best draping performance was E-SP-TR5-W4T1.5, with DCs of 35.8 % along the trace and 57.7 % across the trace. This was 6.04 percentage points lower and 7.28 percentage points higher than the DCs of the baseline along and across the trace, respectively.

**[insert Figure 11 here]**

**[insert Figure 12 here]**

# 4 Conclusions

3D printed traces from three Conductive Composite Filaments (CCF) were investigated in terms of electrical conductivity and drapability for wearable technology applications. The three CCFs, namely 3DK (carbon black/PLA), Protopasta (carbon black/PLA) and Electrifi (copper/polyester), were compared with a baseline textile fabric with a silver yarn trace. 15 straight line (SL) traces with different cross-sections were 3D printed on painter's tape for each CCF (a total of 45 samples). Average values from two multimeters for 2-point resistance measurements were calculated. Electrifi had the best electrical performance while 3DK performed the worst. Protopasta traces demonstrated the most consistent performance across traces with varying cross-sectional area (CSA). The Protopasta and Electrifi traces with the lowest normalized resistance were integrated with textiles in one SL and two S-pattern (SP) geometries. When integrated with a textile fabric, the Electrifi trace was able achieve similar electrical performance to the baseline textile fabric, while Protopasta textile samples displayed much higher normalized resistance. The draping coefficient (DC) for each sample was found using a 3D laser scanner and measuring the undraped and draped area over a pole. This was completed for draping along and across a trace. SP geometries improved the draping performance of the experimental textile samples across the trace. The geometry with a higher turning radius marginally outperformed the SP trace with a lower turning radius, but it came at a cost of a reduction in electrical performance. The SP geometry with a 5 mm turning radius had a normalized resistance of 4.76 Ω/cm and respective DCs of 35.8 % and 57.7 % along and across the trace. The geometry with a 2.5 mm turning radius had a normalized resistance of 3.58 Ω/cm and respective DCs of 45.3 % and 61.07 % along and across the trace. Therefore, if electrical performance is prioritized over drapability, the SP-TR2.5 geometry is the better option. The baseline textile fabric had a normalized resistance of 3.85 Ω/cm, and DCs of 41.9% and 50.4%,

respectively, along and across the silver yarn. As a result, Electrifi traces 3D printed on textile fabric are suitable candidates for wearable technology.

One downside of the Electrifi material was its inconsistent 3D printing performance on textile fabric compared to Protopasta. Therefore, the printing process parameters for the Electrifi CCF could be further improved for integration on a textile fabric surface. The ease of printing and reliability of Protopasta may be useful in applications where the consistency of conductive traces is a higher priority than the resistance of the trace, such as the fabrication of sensors. Factors relating to the durability and longevity of conductive traces 3D printed on textile fabric still require investigation. This includes exploring the bond strength between the 3D printed trace and textile fabric, washability, environmental tests, and stability over time. Micro-CT and other imaging techniques would also allow for the microstructure of the 3D printed traces to be observed and compared. Determining these structural differences would help explain why the resistance of the 3D printed traces changed when extruded on a rigid surface compared to a textile fabric. Overall, this work serves as a preliminary proof of concept that copper/polyester CCFs, such as Electrifi, could be a suitable substitute for textile fabrics that typically utilize silver yarn to impart conductivity. These traces could be used for prototyping circuit designs, interconnects, sensors, and heating elements directly on textile fabric for wearable technology applications.

## Acknowledgements

The authors would like to thank Myant Inc. for supplying the textile fabric used in this work. The authors acknowledge the financial support by the Natural Sciences and Engineering Research Council of Canada (NSERC), RGPIN-2023-04091, and Mitacs and Mitacs accelerate programs, IT13046.

## Conflict of Interest

The authors have no relevant financial or non-financial interests to disclose.

## Data Availability Statement

Data will be made available upon request.

## References

1. E. B. Duoss, M. Twardowski, and J. A. Lewis, Advanced Materials **19**, 3485 (2007).
2. B. Y. Ahn, S. B. Walker, S. C. Slimmer, A. Russo, A. Gupta, S. Kranz, E. B. Duoss, T. F. Malkowski, and J. A. Lewis, Journal of Visualized Experiments (2011).
3. R. H. Sanatgar, A. Cayla, C. Campagne, and V. Nierstrasz, J Appl Polym Sci **136**, (2019).
4. N. Vidakis, M. Petousis, E. Velidakis, N. Mountakis, P. E. Fischer-Griffiths, S. Grammatikos, and L. Tzounis, Journal of Carbon Research **7**, 52 (2021).
5. R. Taherian and A. Kausar, "Electrical Conductivity in polymer-based composites: experiments, modelling, and applications", William Andrew, 2018.
6. P. F. Flowers, C. Reyes, S. Ye, M. J. Kim, and B. J. Wiley, Addit Manuf **18**, 156 (2017).
7. D. Robin, N. Thomas, R. Laurane, F. T. Juan Carlos, R. Colin, T. H. Thuy Quynh, and M. H. Francisca, J Mater Sci **58**, 13118 (2023).
8. K. Sima, D. Kalas, R. Soukup, J. Reboun, and A. Hamacek, in *Proceedings of the International Spring Seminar on Electronics Technology* (IEEE Computer Society, 2022).

9. L. K. Saharan and T. Agbesoyin, in *SPIE 12046, Sensors and Smart Structures Technologies for Civil, Mechanical, and Aerospace Systems* (SPIE-Intl Soc Optical Eng, Long Beach, United States, 2022), p. 1204612.
10. A. Komolafe, B. Zaghari, R. Torah, A. S. Weddell, H. Khanbareh, Z. M. Tsikriteas, M. Vousden, M. Wagih, U. T. Jurado, J. Shi, S. Yong, S. Arumugam, Y. Li, K. Yang, G. Savelli, N. M. White, and S. Beeby, IEEE Access **9**, 97152 (2021).
11. P. Veske-Lepp, B. Vandecasteele, F. Thielemans, V. De Glas, S. Delaplace, B. Allaert, K. Dewulf, A. Depré, and F. Bossuyt, Sensors **24**, (2024).
12. S. Guridi, M. Iannacchero, and E. Pouta, in Conference on Human Factors in Computing Systems - Proceedings (Association for Computing Machinery, 2024).
13. N. Y. K. Lam, J. Tan, A. Toomey, and K. C. J. Cheuk, Fashion and Textiles **9**, (2022).
14. X. Luo, H. Tan, and W. Wen, Bioengineering **11**, (2024).
15. D. Powell and A. Godfrey, NPJ Digit Med **6**, (2023).
16. V. R. Lee and R. B. Shapiro, in (2019), pp. 113–133.
17. C. W. Kan and Y. L. Lam, Applied Sciences (Switzerland) **11**, (2021).
18. A. Ç. Seçkin, B. Ateş, and M. Seçkin, Applied Sciences (Switzerland) **13**, (2023).
19. H. Bruch, A. G. Hahn, R. J. N. Helmer, C. MacKintosh, I. Blanchonette, and M. J. McKenna, in *Procedia Eng* (Elsevier Ltd, 2011), pp. 445–450.
20. J. Azoulay, *Anisotropy in Electric Properties of Fabrics Containing New Conductive Fibers* (1988).
21. R. Orban and S. Applications Engineer, *New Metal-Coated Fibers and Fabric Lead to Novel, Practical Products* (1989).
22. E. R. Post and M. Orth, in *Digest of Papers. First International Symposium on Wearable Computers* (IEEE, 1997), pp. 167–168.
23. A. Tognetti, F. Lorussi, M. Tesconi, and D. De Rossi, in *Proceedings of IEEE Sensors, 2004* (Piscataway NJ: IEEE, 2004), pp. 527–530.
24. M. Stoppa and A. Chiolerio, Sensors (Switzerland) **14**, 11957 (2014).
25. Z. Ahmed, R. Torah, K. Yang, S. Beeby, and J. Tudor, Smart Mater Struct **25**, (2016).
26. G. Goncu-Berk, IOP Conf Ser Mater Sci Eng **1266**, 012001 (2023).
27. R. Silvestre, E. Garcia-Breijo, J. Ferri, I. Montava, and E. Bou-Belda, Polymers (Basel) **15**, (2023).
28. P. A. Eutionnat-Diffo, Y. Chen, J. Guan, A. Cayla, C. Campagne, X. Zeng, and V. Nierstrasz, Rapid Prototyp J **26**, 390 (2020).
29. M. Gandler, F. Eibensteiner, and J. Langer, in *International Conference on Information and Digital Technologies (IDT)* (IEEE, Zilina, Slovakia, 2019), pp. 153–157.
30. N. Grimmelsmann, Y. Martens, P. Schäl, H. Meissner, and A. Ehrmann, Procedia Technology **26**, 66 (2016).
31. S. Kabir, Y. Li, M. Salahuddin, and Y. A. Lee, Clothing and Textiles Research Journal (2023).
32. J. Kalman, K. Fayazbakhsh, and D. Martin, Textile Research Journal **91**, 2387 (2021).
33. T. Spahiu, S. Fafenrot, N. Grimmelsmann, E. Piperi, E. Shehi, and A. Ehrmann, in *IOP Conf Ser Mater Sci Eng* (Institute of Physics Publishing, 2017).
34. T. Spahiu, Z. Zlatev, E. Ibrahimaj, J. Ilieva, and E. Shehi, Machines **10**, (2022).
35. 3DK.Berlin, https://3dk.berlin/en/special/169-3dkonductive.html [Accessed 18 July 2025] (2015).
36. Protopasta, (2020).
37. Protoplant, 3 (2025).
38. Multi3D, Https://Www.Multi3dllc.Com/Faqs/ [Accessed 23 April 2024] (2024).
39. Multi3D LLC, MATERIAL SAFETY DATA SHEET - Electrifi Conductive 3D Printer Filament (Durham, NC, 2016).
40. ISO/ASTM 52902:2019, International Organization for Standardization/American Society for Testing and Materials 1 (2019).
41. P. L. Rossiter, in *The Electrical Resistivity of Metals and Alloys* (Cambridge University Press, Cambridge, 1987), pp. 1–29.

42. M. Nowka, K. Ruge, L. Schulze, K. Hilbig, and T. Vietor, Polymers (Basel) **16**, (2024).
43. Q.-Y. Wei, Y.-D. Fang, Z.-B. Sun, Y. Zeng, J. Zhang, J. Lei, L. Xu, H. Lin, G.-J. Zhong, and Z.-M. Li, Composites Part A: Applied Science and Manufacturing, **169**, 107516 (2023).
44. Z. Tang, H. Kang, Z. Shen, B. Guo, L. Zhang, D. Jia, Macromolecules **45** (2012).
45. J. Li, Y. Li, Z. Wang, H. Bian, Y. Hou, F. Wang, G. Xu, B. Liu, and Y. Liu, Sci Rep **6**, (2016).
46. B. Tormos, S. Ruiz, J. Alvis-Sanchez, and L. I. Farfan-Cabrera, Batteries **10**, (2024).
47. D.V. Ceretti, M. Edeleva, L. Cardon, and D.R. D'hooge, Molecules **28**, (2023).
48. A. Sabalina, S. Gaidukovs, O. Platnieks, O. Starkova, G. Gaidukova, L. Orlova, and M. Jurinovs, RSC Sustainability, (2025).

**Table 1. A summary of the best experimental results in the literature on the electrical performance of 3D printed structures integrated with textiles and draping performance of 3D printed textile structures.**

| Source | Material | Structure | Dimensions | Normalized Resistance | Draping Coefficient |
|---|---|---|---|---|---|
| Sima et al. [8] | Electrifi (Copper/Polyester) | 3D printed triangular trace integrated with textile using thermo-compression. | 100 mm – length<br>0.08 $mm^2$ – CSA | 3.3 $\Omega$/cm | N/A |
| Goncu-Berk [26] | NinjaTek Eel (Conductive TPU) | Rectangular trace 3D printed on a polyester knitted textile. | 10 mm – length<br>4 $mm^2$ – CSA | 18.2 k$\Omega$/cm | N/A |
| Gandler et al. [29] | PI-ETPU (Carbon black/TPU) | Rectangular trace 3D printed on textile, then ironed. | 70 mm – length<br>N/A – CSA | 109 k$\Omega$/cm | N/A |
| Grimmelsmann et al. [30] | Protopasta (Carbon black/PLA) | Rectangular trace 3D printed on textile. | 250 mm – length<br>10 $mm^2$ – CSA | ~100 $\Omega$/cm | N/A |
| Kabir et al. [31] | Engineering TPU filament | 3D printed auxetic textile. | 200 mm – diameter<br>0.4 mm – thickness | N/A | 26.8 % |
| Kalman et al. [32] | White TPU | 3D printed iso-grid textile. | 100 mm – diameter<br>0.25 mm – thickness | N/A | 21.9 % |
| Spahiu et al. [34] | PLA | Small PLA circles 3D printed on linen textile. | N/A | N/A | 36 % |
| This study | Electrifi (Copper/Polyester) | rectangular prism in an S-pattern 3D printed on textile. | 115 mm – end-to-end length<br>6 $mm^2$ – CSA | 3.58 $\Omega$/cm | 45.3 % - along trace<br>61.1 % - across trace |

Abbreviations: CSA, cross-sectional area

**Table 2. Conductive composite filaments**

| Filament | Composition | Density ($g/cm^3$) | Resistivity (Ω.cm) | Melting Point (°C) |
|---|---|---|---|---|
| 3Dkonductive [35] | Carbon Black/PLA | N/A | 24 | 154* |
| Protopasta [36, 37] | Carbon Black/PLA | 1.15 | 30 (x/y-direction)<br>115 (z-direction) | ~ 155 |
| Electrifi [38, 39] | Copper/Polyester | 2.5 | 0.006 | ~ 60 |

* A Differential Scanning Calorimetry (DSC) test was performed in this study to find this value.

**Table 3. 3D printing process parameters used for each CCF.**

| Filament | Belkin-3DKonductive | Protopasta | Electrifi |
|---|---|---|---|
| **Bed Temp (°C)** | 60 | 60 | 20 |
| **Infill percentage (%)** | 100 | 100 | 100 |
| **Print Speed (mm/s)** | 60 | 35 | 30 |
| **Nozzle Temp (°C)** | 215 | 215 | 142 |
| **Extrusion Ratio (%)** | 100 | 100 | 102 |
| **Layer Height (mm)** | 0.2 | 0.2 | 0.24 |

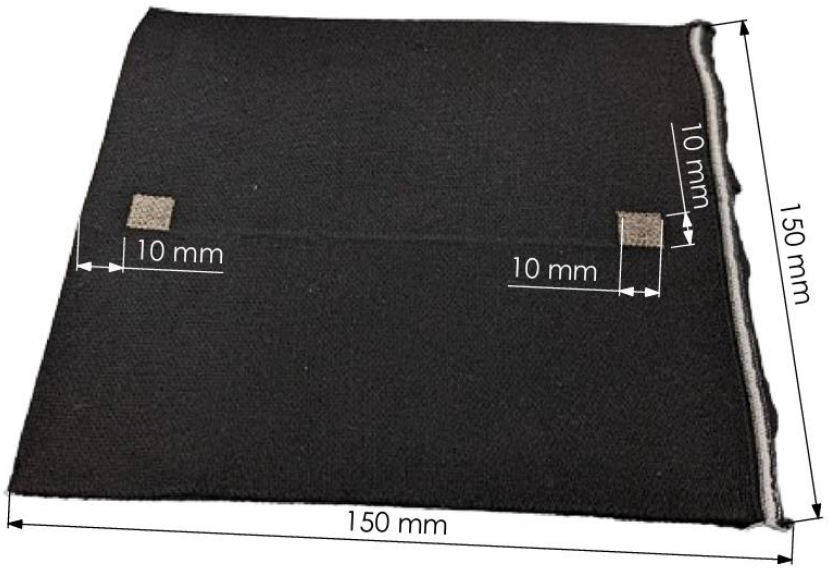


**Figure 1. Baseline textile fabric sample with integrated silver yarn conductive trace.**

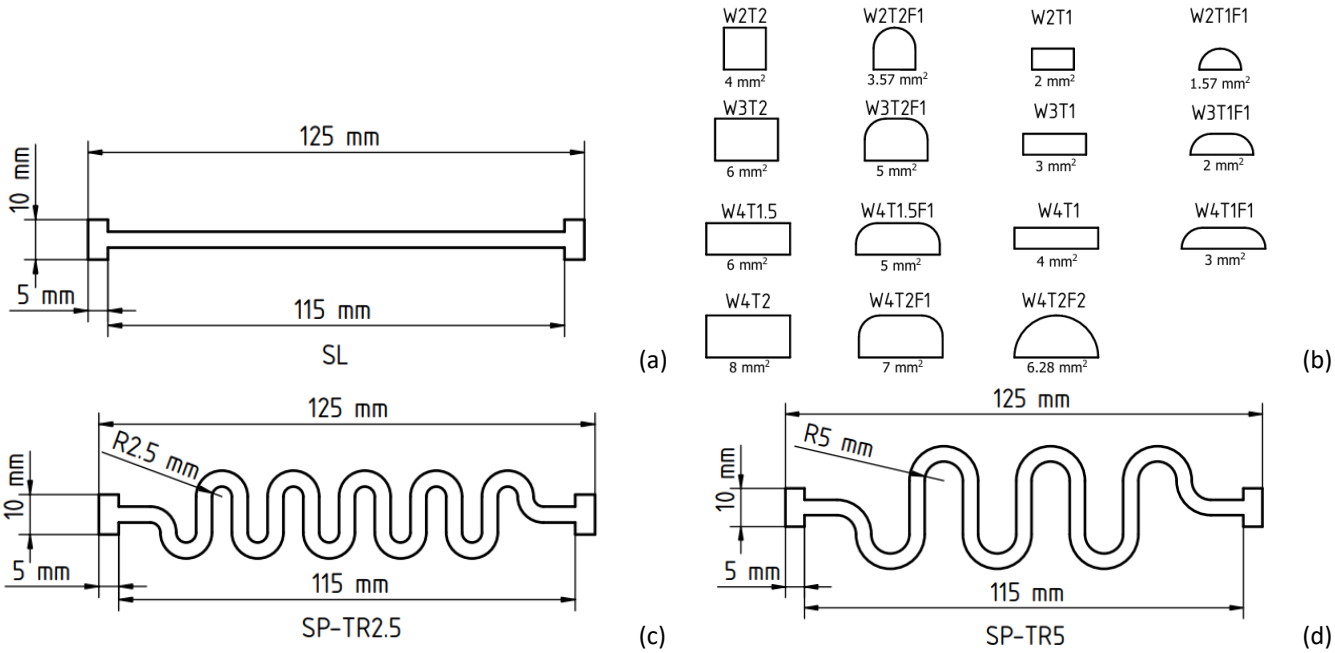


**Figure 2. Trace geometries: (a) SL; (b) different CSAs with their cross-sectional areas; (c) SP-TR2.5; and (d) SP-TR5.**


**Figure 3. 3D-printed trace integrated on a textile fabric demonstrating the method used for alignment and securing the textile to the build platform.**


**Figure 4. Electrifi SL traces 3D printed on painter's tape with silver conductive epoxy after curing in the dehydrator.**


**Figure 5. E-SP-TR2.5-W4T1.5 textile sample being measured for drapability across the 3D printed trace.**

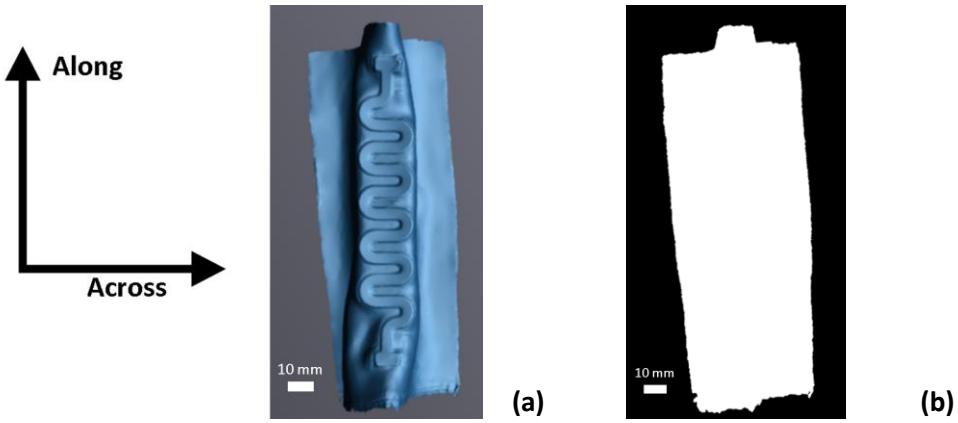


**Figure 6. 3D scan of E-SP-TR2.5-W4T1.5 textile sample draped along the 3D printed trace: (a) before; and (b) after image processing.**

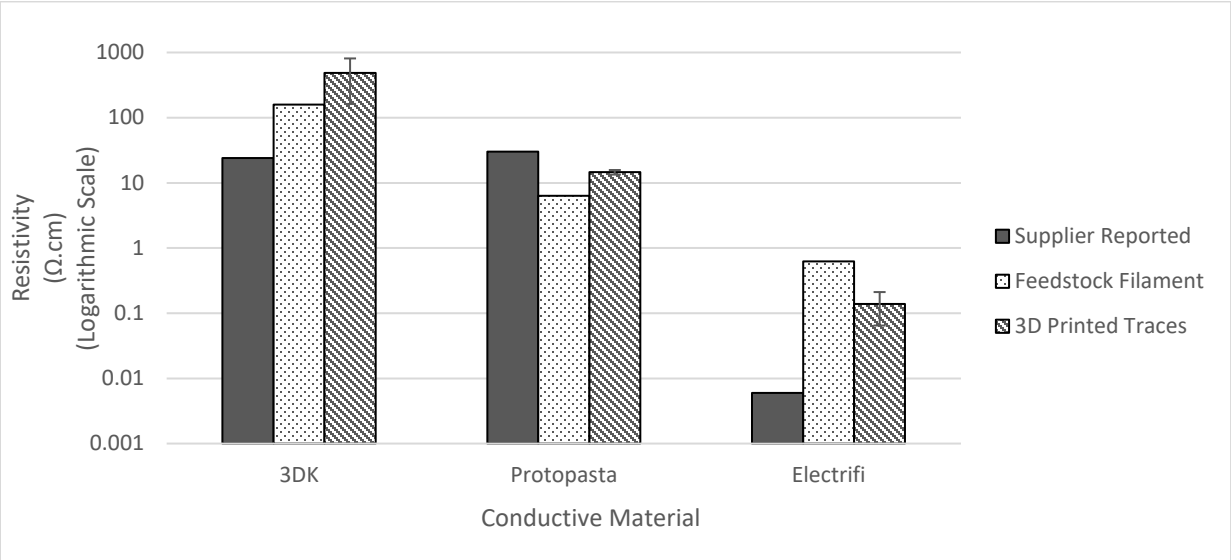


**Figure 7. Resistivity of the CCFs according to the supplier, feedstock filament, and 3D printed SL traces. Error bars represent one standard deviation.**

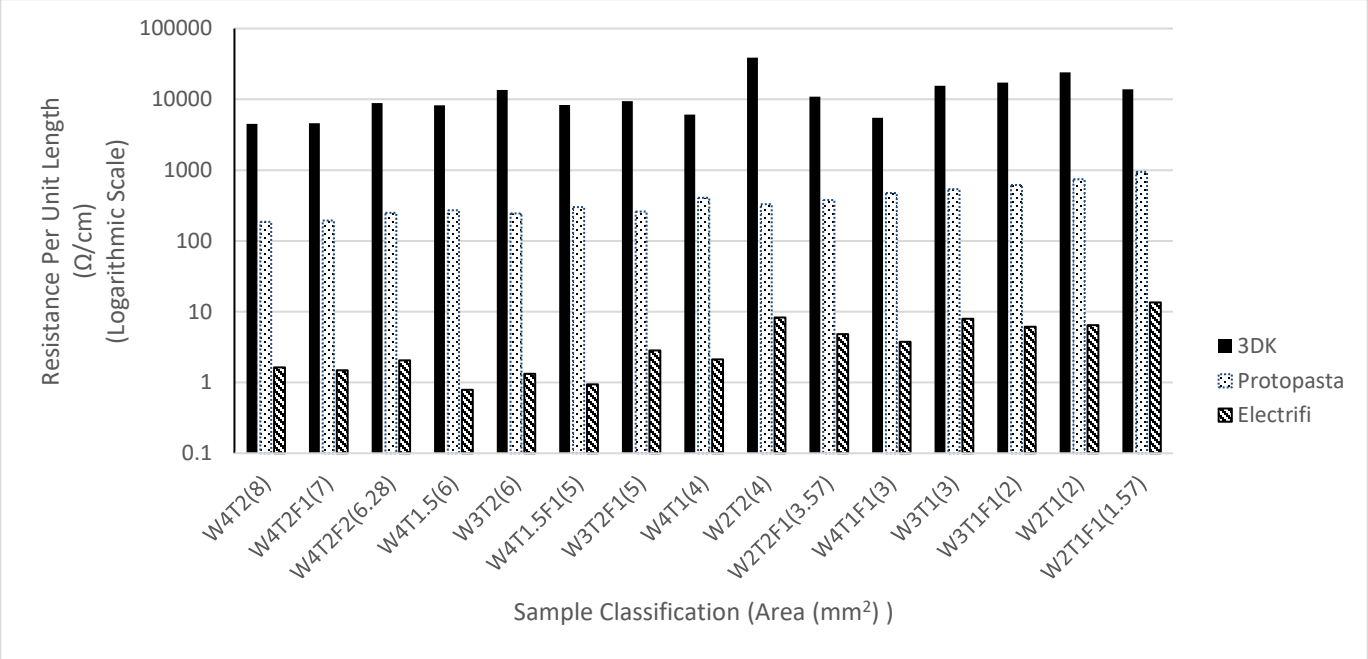


**Figure 8. The effect of the trace geometry on the normalized resistance of SL traces made from 3DK, Protopasta, and Electrifi CCFs. Resistance was normalized over a 1 cm length. The CSA for each trace geometry is provided in parentheses following the trace designation.**

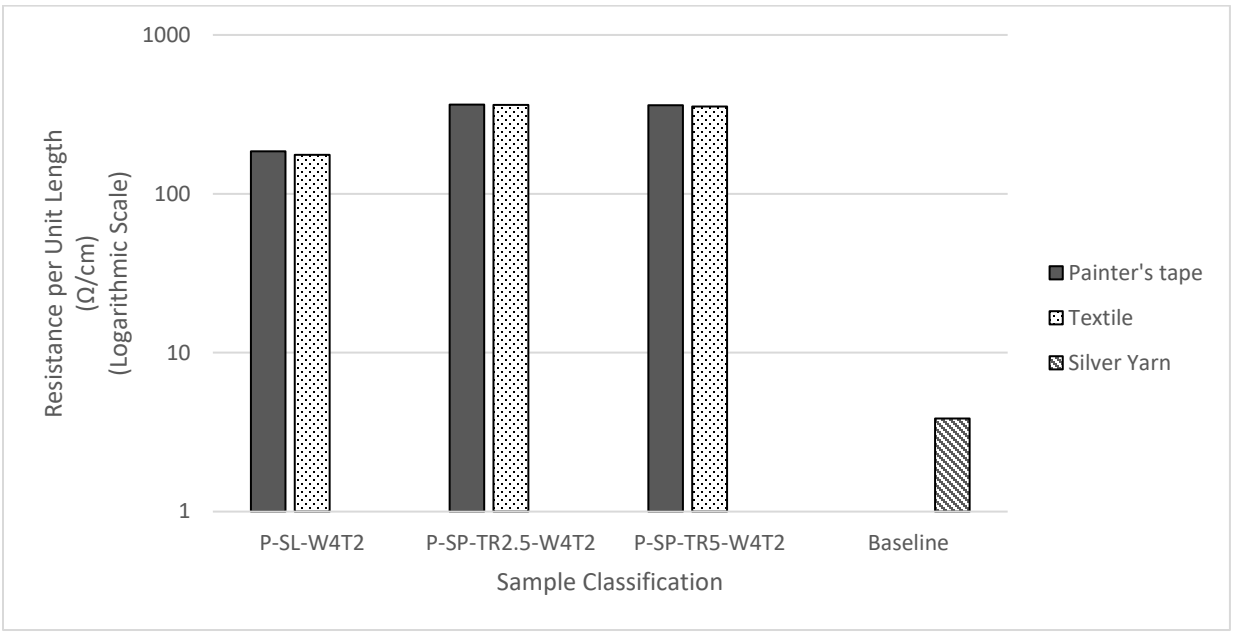


**Figure 9. Normalized resistance of different Protopasta trace geometries 3D printed on painter's tape and textile fabric compared to the silver yarn baseline.**

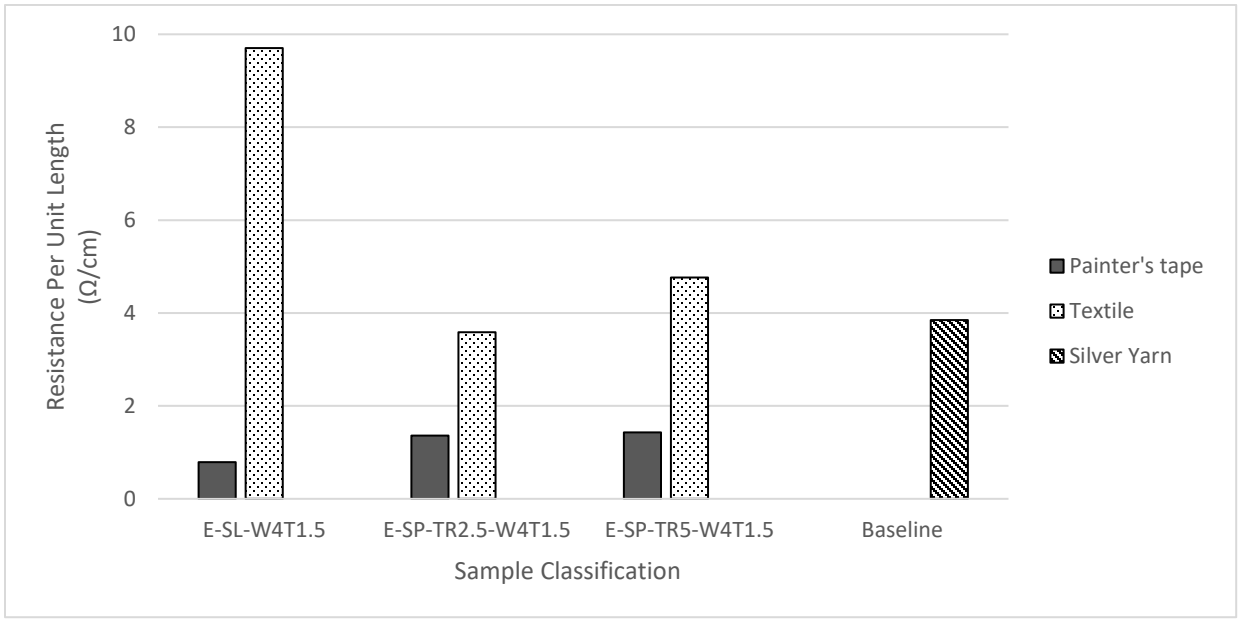


**Figure 10. Normalized resistance of different Electrifi trace geometries 3D printed on painter's tape and textile fabric compared to the silver yarn baseline.**

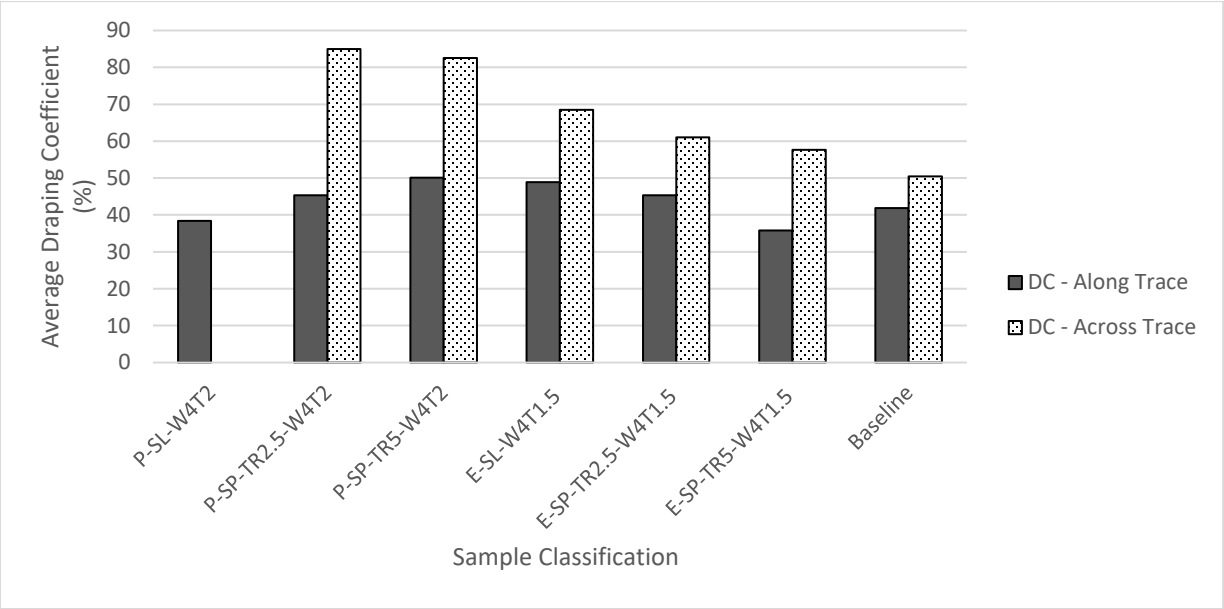


**Figure 11. Drapability along and across the trace for the Protopasta (P), Electrifi (E), and baseline samples.**

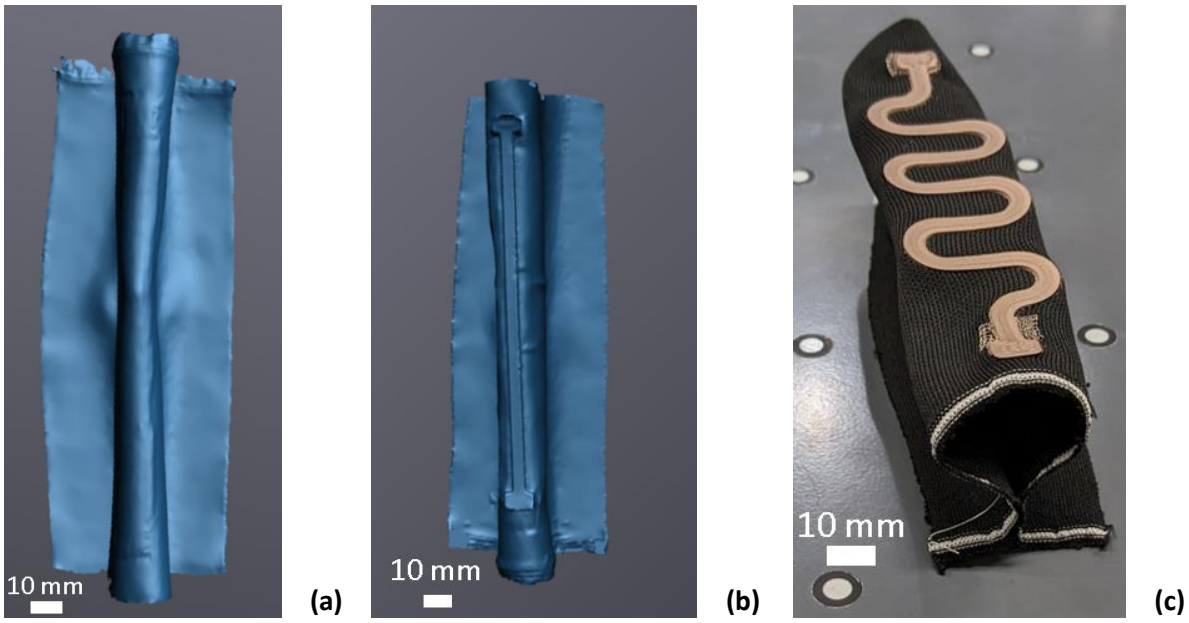


**Figure 12. Drapability of the textiles along the trace: (a) baseline sample; (b) P-SL-W4T2; and (c) E-SP-TR5-W4T1.5 sample.**